JOURNAL OF QUATERNARY SCIENCE (2019) **34**(2) 101–111 ISSN 0267-8179. DOI: 10.1002/jqs.3084

JQS Journal of Quaternary Science QRA Quaternary Research Association

Evolution of the relative abundance of C_4 plants on the Chinese Loess Plateau since the Last Glacial Maximum and its implications

WENQI JIANG,[1,3] JIANYU WU,[1] HAIBIN WU,[1,2,3]* QIN LI,[1,4] YATING LIN[1,3] and YANYAN YU[1,2]

[1]Key Laboratory of Cenozoic Geology and Environment, Institute of Geology and Geophysics, Chinese Academy of Sciences, Beijing, China

[2]CAS Center for Excellence in Life and Paleoenvironment, Beijing, China

[3]University of Chinese Academy of Sciences, Beijing, China

[4]CAS Center for Excellence in Tibetan Plateau Earth Sciences, Beijing, China

Received 11 July 2018; Revised 20 November 2018; Accepted 6 December 2018

ABSTRACT: Understanding the distribution of C_3 and C_4 plants and its forcing mechanisms since the Last Glacial Maximum (LGM) is important for anticipating their possible response to future climate change. The spatiotemporal pattern of C_4 plant abundance on the Chinese Loess Plateau (CLP) is complex and the dominant causal factors are contentious. Here, we use $\delta^{13}C$ records of organic matter in paleosols from the CLP to reconstruct changes in the representation of C_4 plants since the LGM. The results indicate that the relative abundance of C_4 plants increased after the LGM, reaching a maximum during 10–6 ka bp, and then decreased. Spatially, the representation of C_4 plants was characterized by increasing values from north-west to south-east. In addition, the smallest spatial difference (~10%) in the representation of C_4 plants between the north-west and south-east parts of the CLP was during the LGM, and the largest difference (~30%) was during the early Holocene. We combined our findings with output from the BIOME4 model to study the sensitivity of C_4 plants to changes in climate and atmospheric CO_2 concentration. The results suggest that increasing temperature was the dominant factor driving C_4 plant expansion on the CLP since the LGM. © 2019 John Wiley & Sons, Ltd.

KEYWORDS: BIOME4; C_3/C_4 plants; Chinese Loess Plateau; organic carbon isotope; temperature.

Introduction

The IPCC 5th report (Stocker *et al.*, 2013) indicates that average global temperature will increase by 1.1–2.6 °C by the end of the present century, which will significantly affect terrestrial ecosystems. C_3 and C_4 plants are the most important components of terrestrial ecosystems (Sage *et al.*, 1999), and the relative abundance of C_3 and C_4 plants depends strongly on both the atmospheric CO_2 concentration and seasonal climate change (Ehleringer *et al.*, 1997; Sage *et al.*, 1999). C_4 plants are favored under lower pCO_2 conditions when accompanied by elevated temperatures (Cerling *et al.*, 1997). Therefore, the impact of global warming on changes in C_3 and C_4 plants has been the subject of intensive investigation in recent years.

The Last Glacial Maximum (LGM) was the last time during the last glacial period when ice sheets were at their maximum extent (Clark *et al.*, 2009), and reconstructed global surface temperatures were ~4–5 °C lower than today (e.g. Bartlein *et al.*, 2011; Shakun *et al.*, 2012). The warming interval from the LGM to the Holocene was accompanied by abrupt warming/cooling events and significant changes in atmospheric CO_2 concentration (Masson-Delmotte *et al.*, 2013). Climate reconstructions also indicate that Northern Hemisphere annual temperature during the early and middle Holocene was ~0.8–1 °C higher than at present (Shakun *et al.*, 2012; Marcott *et al.*, 2013), which is comparable to projected climatic conditions in the future, given ongoing global warming. Thus, understanding changes in the relative abundance of C_3 and C_4 plants since the LGM may help anticipate their responses to future climate change.

The Chinese Loess Plateau (CLP) is located in the marginal zone of the region of influence of the East Asian summer monsoon. The climatic gradient is steep (Qian, 1991) and thus the area is sensitive to climatic changes. The continuous loess–paleosol sequences of the CLP are valuable archives for investigating the evolution of terrestrial ecosystems (Liu, 1985). Studies of the carbon isotope composition of soil organic matter (SOM) and leaf wax n-alkanes from the loess–paleosol sequences indicate that the relative abundance of C_4 plants generally increased from the LGM to the Holocene (e.g. Gu *et al.*, 2003; Zhang *et al.*, 2003; Liu *et al.*, 2005a; Yang *et al.*, 2015), but the spatiotemporal pattern of variation was significantly different. Therefore, the nature of the spatiotemporal evolution of C_4 abundance on the CLP since the LGM is an important unresolved issue. Furthermore, there is debate regarding whether an enhanced East Asian monsoon (Vidic and Montañez, 2004; Liu *et al.*, 2005a; Yang *et al.*, 2015) or increasing temperature (Gu *et al.*, 2003; Zhang *et al.*, 2003; Rao *et al.*, 2012) was the dominant influence on C_4 expansion. Therefore, the relative importance of these factors needs to be investigated in more detail to improve our understanding of the main driver of C_4 expansion in the region.

Here, we use a synthesis of carbon isotope records of SOM from 28 loess–paleosol sequences since the LGM, and of modern surface soils across the CLP, to characterize the spatiotemporal pattern of changing C_4 abundance. Subsequently, we used a vegetation model, BIOME4 (Kaplan *et al.*, 2003; Hatté and Guiot, 2005), based on the physiological

*Correspondence: Haibin Wu, [1]Key Laboratory of Cenozoic Geology and Environment, as above.
E-mail: haibin-wu@mail.iggcas.ac.cn

responses of C_3 and C_4 plants to changing atmospheric CO_2 levels and climate changes, to improve our understanding of the forcing mechanisms of C_4 plant expansion, and to elucidate the effects of temperature, precipitation and atmospheric CO_2 concentration on changes in C_3 and C_4 abundance on the CLP.

Regional setting

The CLP is located in northern China (Fig. 1), which experiences temperate, arid and semi-arid climati conditions (Sheng, 1986; Qian, 1991). Thus, the region provides an excellent opportunity to evaluate the interactions between changing climatic conditions and vegetation. The climate is dominated by the alternating East Asian winter and summer monsoons (Chen *et al.*, 1991). Cold-dry north-west winds control the region in the winter season, and the warm-humid south-east summer monsoon penetrates further inland during the summer season, supplying 38–65% of the annual rainfall (Qian, 1991).

Mean annual precipitation and temperature vary systematically across the CLP, ranging, respectively from 200 mm and 8 °C in the north-west to 700 mm and 14 °C in the south-east (Fig. S1). The present vegetation is mainly dominated by semi-arid grasses and shrubs comprising both C_3 and C_4 plants. *Stipa bungeana* and *Lespedeza davurica* are common C_3 plants and *Bothriochloa ischaemum* is a common C_4 grass (Yin and Li, 1997; Wang, 2001).

Materials and methods

Data and chronology

The C_3 and C_4 photosynthetic pathways result in fractionation of carbon isotopes to differing degrees, with corresponding $\delta^{13}C$ ranges of about −22 to −30 and −10 to −14‰ (e.g. Bender, 1971; Farquhar, 1983). The $\delta^{13}C$ values of SOM reflect the carbon isotopic composition of the organic matter derived from C_3 and C_4 plants with little or no isotopic fractionation (Melillo *et al.*, 1989; Wang *et al.*, 2008). Thus, they are a reliably proxy for tracing changes in the composition of the parent vegetation (Schwartz *et al.*, 1986; Cerling, 1999; Hatté *et al.*, 2001).

In this study, we assembled previously published $\delta^{13}C$ records of SOM from loess–paleosol sequences of the CLP. The $\delta^{13}C$ records were selected based on the following criteria: (i) record length spanned most of the last 21 ka bp; (ii) a magnetic susceptibility record was available for the same section, enabling high-resolution stratigraphic correlation (Heller and Liu, 1984); and (iii) sampling resolution was better than 1000 years. Based on these criteria, 28 loess sites were selected (Fig. 1; Table S1). In addition, modern surface soil $\delta^{13}C$ data ($n = 34$) were assembled from Wang (2001) and Liu *et al.* (2002).

Optically stimulated luminescence (OSL) dating allows the direct and accurate determination of the burial ages of lithogenic sediments and has been widely applied to Chinese loess–paleosol sequences (Stevens and Lu, 2009; Kang *et al.*, 2011, 2013). A high-precision chronology was constructed for the Weinan loess section (designated Weinan-1) on the CLP (Kang *et al.*, 2011, 2013) based on high-resolution quartz OSL dating (at 10–20-cm intervals). In addition, additional OSL dating results were available for Xifeng (designated Xifeng-1, Lu *et al.*, 2006a), Luochuan (Luochuan-1, Lu *et al.*, 2007), Lantian (Lantian-1, Lu *et al.*, 2006b) and Yuanbao (Yuanbao-1, Lai and Wintle, 2006).

The loess–paleosol sequences of the CLP are readily correlated, especially on the basis of their magnetic susceptibility variations, which can be matched in detail from site to site across the plateau, and thus they can be used as a high-resolution stratigraphic tool (Heller and Liu, 1984). We correlated the magnetic susceptibility record of the Weinan-1 section, for which a high-resolution OSL chronology was available, with the magnetic susceptibility records of 20 of our selected sites in this study. This enabled seven age control

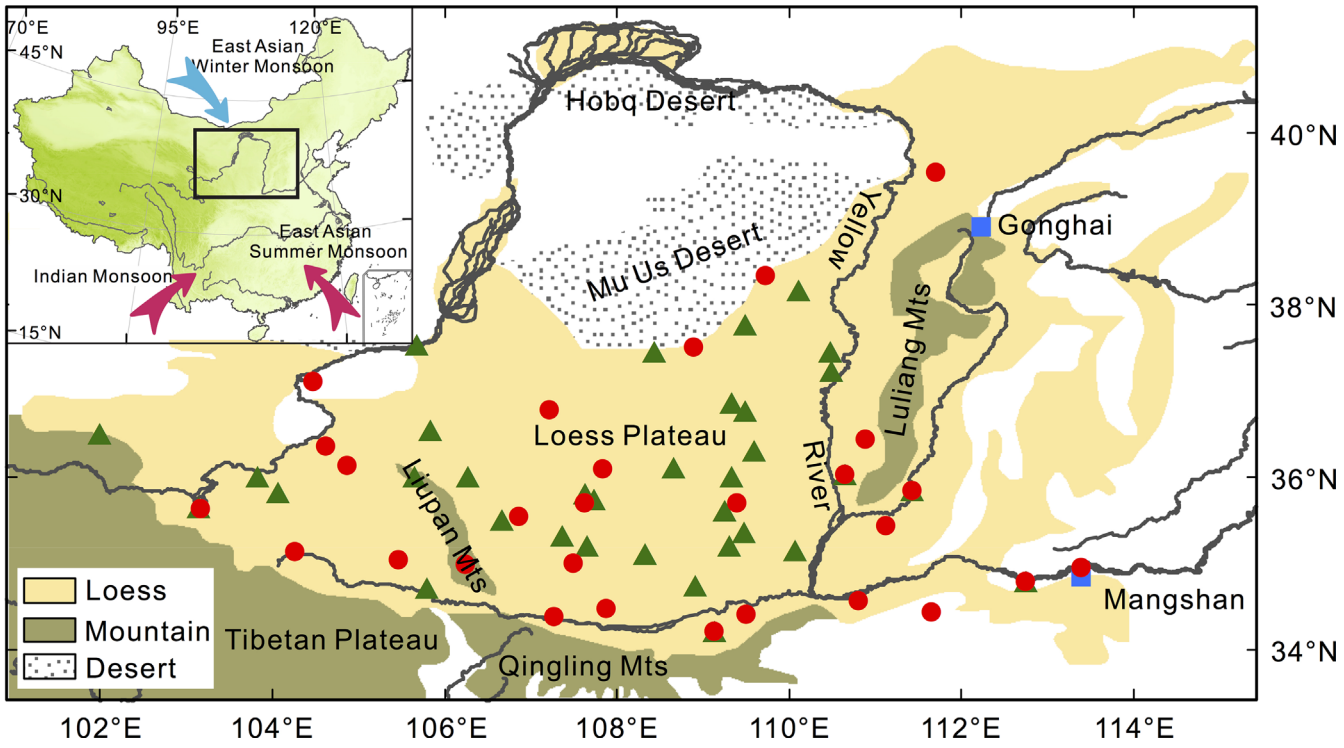

Figure 1. Map of the Chinese Loess Plateau, prevailing monsoon circulation and study sites. Red dots represent the locations of the studied loess–paleosol sequences and green triangles represent surface soil sites. Arrows in the inset map indicate the direction of the winter and summer monsoonal winds.

points to be applied to the stable carbon isotope records used in the study (see Text S1 and Fig. S2 for details).

Age models for five sites (Luochuan, Xifeng, Qingyang, Lantian and Yuanbao) were established based on correlations with nearby sections with reliable OSL chronologies (see Text S1 and Fig. S2 for details). The chronologies of the other three sites, Jingyuan (Liu *et al.*, 2011), Yulin (Lu *et al.*, 2013) and Liangjiacun (Tan *et al.*, 2015), were constructed based on their respective OSL ages, which are independent and objective; thus, we did not need to correlate them with other OSL-based chronologies.

The ages of the sediment depths between the age control points were then estimated by interpolation using a magnetic susceptibility model (Kukla *et al.*, 1988; Kukla and An, 1989). Consequently, independent high-resolution timescales for the selected sections for the past 21 ka bp were obtained. Although this chronology, based on magnetic susceptibility correlations, may lead to some degree of error, we consider it acceptable for the analysis of environmental changes on an orbital timescale.

A novel aspect of this study was the application of a physiological process-based vegetation model, BIOME4 (Kaplan *et al.*, 2003; Hatté and Guiot, 2005), to study the sensitivity of C_3 and C_4 plants to changes in climate and atmospheric CO_2 since the LGM. Model inputs included data on soil textural class, absolute minimum temperature, atmospheric CO_2 concentration and monthly climate (temperature, precipitation and insolation). In this study, the modern atmospheric CO_2 concentration was set to 380 ppmv, because most of the modern plants and surface soil samples were collected during the 2000s. The soil properties were derived from the FAO digital soil map of the world (Food and Agriculture Organization (FAO), 1995). The modern monthly climate dataset and absolute minimum temperatures were compiled by the Chinese Central Meteorological Office. The artificial neural network technique was used to interpolate the modern monthly climate conditions and absolute minimum temperatures (Guiot *et al.*, 1996).

Reconstruction of the relative abundance of C_3 and C_4 plants

To estimate the relative abundance of C_3 and C_4 plants, it is essential to determine the respective end-member $\delta^{13}C$ values. Previous studies have revealed that the $\delta^{13}C$ values of C_3 and C_4 plants are affected by the atmospheric CO_2 concentration, the $\delta^{13}C$ of atmospheric CO_2 ($\delta^{13}C_{atm}$), precipitation and temperature (Farquhar *et al.*, 1989; Brugnoli and Farquhar, 2000). During the past 21 ka bp, $\delta^{13}C_{atm}$ was positive by 1.7–1.4‰ compared to that of the present-day. This is largely due to the incorporation of atmospheric CO_2 that is depleted in ^{13}C from fossil fuel combustion, and changes in isotopic fractionation during air/sea gas exchange (Freyer and Belacy, 1983; Schmitt *et al.*, 2012). Here, we assumed a mean value of 1.55‰ for the $\delta^{13}C_{atm}$ correction (Table 1).

Coefficients of −0.40‰/100 mm and 0.104‰/°C have been reported for the relationship of C_3 plants to respective changes in precipitation and temperature on the CLP (Wang *et al.*, 2008, 2013); however, these coefficients are negligible for C_4 plants (Wang *et al.*, 2008, 2013). During the LGM, reconstructed precipitation and temperature on the CLP were lower by ~100–300 mm and ~7 °C, respectively, compared to today (Wu *et al.*, 2002; Peterse *et al.*, 2011). In this case, the combined effect of climate change on the $\delta^{13}C$ values of C_3 plants would be about −0.3 to 0.5‰. During the mid-Holocene, the reconstructed precipitation and temperature values were higher than present by ~130 mm and by ~2–4 °C, respectively (Shi *et al.*, 1992; Chen *et al.*, 2015); the net effect of these differences on C_3 plants would be about −0.3 to −0.1‰. Hence, even during these two intervals of relatively extreme climatic conditions, the effects of climate on the $\delta^{13}C$ values of C_3 plants were probably insignificant. Consequently, we ignored the effect of climate changes since the LGM on the $\delta^{13}C$ of C_3 plants. In addition, we also ignored the effect of changes in atmospheric CO_2 concentration, because carbon isotope discrimination in C_3 plants may be independent of natural variations in CO_2 concentration on geological timescales (Diefendorf *et al.*, 2015; Kohn, 2016; Voelker *et al.*, 2016).

Soils show progressive enrichment in the ^{13}C content of SOM irrespective of changes in vegetation type (C_3 and C_4) due to microbial degradation. An ~1.0‰ increase in the ^{13}C value of SOM compared to above-ground vegetation has been documented (Melillo *et al.*, 1989). After correcting for the effect of $\delta^{13}C_{atm}$ and for SOM degradation, we tentatively adopted respective end-member $\delta^{13}C$ values of C_3 and C_4 plants of −24.1 and −10.0‰ for the past 21 ka bp (Table 1). Estimated C_4 plant abundance was then calculated using the isotope mass-balance equation:

$$C_4(\%) = \frac{\left(\delta^{13}C - \delta^{13}C_{C3}\right)}{\delta^{13}C_{C4} - \delta^{13}C_{C3}} \times 100$$

where $\delta^{13}C_{C3}$ and $\delta^{13}C_{C4}$ are the end-member $\delta^{13}C$ values of C_3 and C_4 plants; $\delta^{13}C$ is the $\delta^{13}C$ of SOM; and $C_4(\%)$ is the relative abundance of C_4 plants in the local environment.

The spatiotemporal variation of C_4 abundance was reconstructed for each 1000-year time slice. Temporal changes in $\delta^{13}C$ values and C_4 abundance were estimated by averaging the $\delta^{13}C$ values of the 28 sites (e.g. the values for 1 ka bp were the means during 0.5–1.5 ka bp, etc.). Contour maps of $\delta^{13}C$ values and C_4 abundance were created using Golden Surfer (Surfer Access System version 12.0, Golden Software, Inc., Golden, CO, USA). To generate isolines that had the property of minimum total curvature, a minimum curvature method was applied; the algorithm can produce a grid with a high degree of internal consistency (Briggs, 1974).

Table 1. Calculation of end-member $\delta^{13}C$ values for C_3 ($\delta^{13}C_{C3}$) and C_4 plants ($\delta^{13}C_{C4}$) on the CLP since the LGM.

Factor	$\delta^{13}C_{C3}$ (‰)	$\delta^{13}C_{C4}$ (‰)	References
Modern vegetation	−26.7	−12.6	Wang *et al.* (2003, 2006, 2008); Liu *et al.* (2005b)
$\delta^{13}C_{atm}$ correction (+1.55‰)	−25.1	−11.0	Mauna Loa Observatory 2000; Schmitt *et al.* (2012)
Degradation correction (+1.0‰)	−24.1*	−10.0	Melillo *et al.* (1989)

*Note that the net effect of temperature and precipitation would range from ~−0.3 to 0.5‰ for the LGM and from −0.3 to −0.1‰ for the mid-Holocene (see 'Reconstruction of the relative abundance of C_3 and C_4 plants). If we assume the net effect is −0.3‰, the C_4 abundance estimated in this study may be underestimated by ~1.5%. Alternatively, if the net effect is 0.5‰, the C_4 abundance estimated in this study may be overestimated by ~3.5%. Thus, this small degree of uncertainty is insignificant and is not corrected for.

Sensitivity analysis of the effects of climate and CO_2 concentration on C_3 and C_4 plants

BIOME4 is an equilibrium vegetation model (Kaplan *et al.*, 2003; Hatté and Guiot, 2005) which considers the effects of CO_2 on net assimilation, stomatal conductance, leaf area index and ecosystem water balance. The model is a significant advance in the simulation of isotopic fractionation produced by C_3 and C_4 plants; it is conceptually related to the model of Lloyd and Farquhar (1994). The maximum potential intercellular-to-atmospheric CO_2 concentration (c_i/c_a) ratio is prescribed for each plant functional type (PFT) and the actual c_i/c_a value is subsequently calculated by iterative optimization. By weighting the monthly fractionation of the C_3 and C_4 plants in all PFTs with their respective net primary production at a given site, the mean annual isotopic fractionation is estimated (Hatté and Guiot, 2005).

To perform a sensitivity analysis to identify the dominant factors controlling the observed changes in C_4 abundance since the LGM, the range of climatic and CO_2 concentration of input parameters used for the BIOME4 model should cover their respective ranges of variation since the LGM. Paleotemperature reconstructions on the CLP have revealed that during the early and mid-Holocene, mean annual temperature (MAT) was up to ~2–4 °C higher than today (Shi *et al.*, 1992; Peterse *et al.*, 2011), while at the LGM it was ~7 °C lower than today (Peterse *et al.*, 2011). During the mid-Holocene, mean annual precipitation (MAP) was ~130 mm greater than today, a difference of ~30% (Chen *et al.*, 2015); by contrast, at the LGM, MAP was ~100–300 mm lower than today, a difference of ~20–50% (Wu *et al.*, 2002). In addition, atmospheric pCO_2 increased from the LGM level of ~180 ppmv to the modern level of ~380 ppmv (Lüthi *et al.*, 2008; Mauna Loa Observatory; Table 2).

Three sensitivity experiments using a single variable method were carried out based on the estimated temperature, precipitation and CO_2 concentration (Table 2): (i) while monthly temperature was increased from −7 °C below to +4 °C above the modern temperature, precipitation and CO_2 were held constant at modern values; (ii) while monthly precipitation was increased from −50% below to +30% above modern precipitation, temperature and CO_2 were held constant at modern values; and (iii) when CO_2 concentration was increased from 180 to 380 ppmv, temperature and precipitation were held constant at modern values.

Results

Spatiotemporal variation of the relative abundance of C_4 plants since the LGM

The $\delta^{13}C$ values of SOM indicate large changes in the relative abundance of C_4 plants since the LGM, from 8.4 to 26.8% (Figs 2 and S3). Mean C_4 abundance was around 10.9% during the glacial period and as high as 22.3% during the Holocene. C_4 abundance remained relatively stable at 8.6% from 21 to 19 ka bp, increased significantly from 16 to 11 ka bp, reached a maximum of 26.1% from 10 to 6 ka bp, and then gradually decreased to 13.5% at the present-day.

The spatial variations in $\delta^{13}C$ values indicate that the distribution of C_4 plants was characterized by an increasing NW–SE trend for all time intervals since the LGM (Figs 3 and S4–S5). C_4 abundance was <~10% in the north-west and increased to ~10–30% towards the south-east during 21–19 ka bp. Thereafter, C_4 abundance increased throughout the Loess Plateau, increasing from ~10–20% in the north-west to ~40–60% in the south-east, during 11–6 ka bp. C_4 percentage values at the present-day increase from ~10–20% in the north-east to ~30% in the south-east.

Table 2. Ranges of parameters used for sensitivity experiments on the CLP since the LGM.

Parameter	Range
ΔT	[−7, +4] °C
ΔP	[−50, +30] %
CO_2 concentration	[180, 380] ppmv

The climate ranges are in terms of the deviation from modern values (degrees for temperature and percentages for precipitation). *T*, mean annual temperature; *P*, mean annual precipitation.

Validation of the BIOME4 model with modern data from the CLP

The BIOME4 simulation of the fractionation of carbon isotopes within the terrestrial biosphere has already been validated by Hatté and Guiot (2005) using modern data from woodland in southern Queensland, Australia (Stewart *et al.*, 1995), and from grassland and woodland along two transects in south-eastern Utah and south-central New Mexico (USA) (Van de Water *et al.*, 2002). However, it remains uncertain whether the BIOME4 model is applicable to the CLP, and therefore it is necessary to evaluate its reliability using the dataset presented here.

Validation was accomplished using the $\delta^{13}C$ values of modern plants and surface soil samples (343 data points from 145 sites, see Table S2 for detailed information) for the CLP. Linear regression analysis was used to compare the simulated $\delta^{13}C$ values at each site compared with the observed values and yielded the following regression equation: $y = 0.9501x - 0.8078$ ($R^2 = 0.91$), where x and y are the observed and simulated values, respectively. The high coefficient of determination and the slope close to unity demonstrate that the BIOME4 model can be applied in the study region.

Impact of climate and atmospheric CO_2 concentration on the relative abundance of C_4 plants

The results of sensitivity experiments to evaluate the response of C_4 plant abundance to changes in temperature, precipitation and CO_2 concentration are shown in Fig. 4. The relative abundance of C_4 plants exhibits a strongly increasing trend from 0.2 to 39.9% when temperature was increased from −7 °C below to +4 °C above modern temperature (Fig. 4, red squares). This indicates that C_4 plants are favored by higher temperatures. By contrast, although C_4 plant abundance increased slightly in the range of low precipitation, it generally decreased by ~1.1% when precipitation was increased from −50% below to +30% above the modern value (Fig. 4, blue triangles). This indicates that lower precipitation favors C_4 plant growth. Similarly, C_4 abundance exhibited a negative shift of ~8.6% when atmospheric CO_2 concentration was increased from 180 to 380 ppmv (Fig. 4, green cycles), indicating that lower CO_2 levels favor C_4 plants.

The results of the three sensitivity experiments indicate that C_4 abundance responded positively to increased temperature and negatively to increased atmospheric CO_2 concentration and precipitation. In addition, it is noteworthy that the percentage of C_4 plants changed more rapidly in response to changes in temperature than to changes in either atmospheric CO_2 concentration or precipitation on the CLP since the LGM.

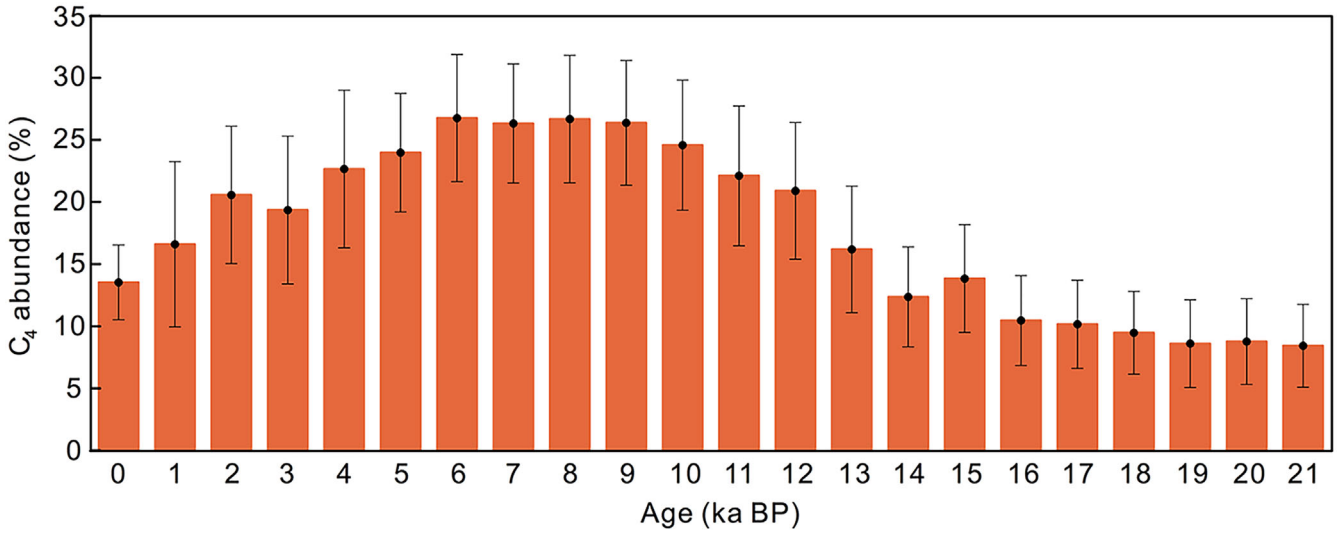

Figure 2. Temporal changes in C_4 abundance on the CLP since the LGM. The values are means, and the error bars represent the 95% confidence interval.

Discussion

Comparison with previous studies

Although several previous studies have investigated temporal changes in the relative abundance of C_3 and C_4 plants at individual sites on the CLP since the LGM (e.g. Vidic and Montañez, 2004; Xie *et al.*, 2004; Liu *et al.*, 2011; Lu *et al.*, 2013), spatial changes have rarely been addressed. Moreover, while several studies have presented distribution patterns of C_4 plants for the LGM and mid-Holocene intervals for the CLP and have shown that C_4 plant abundance was characterized by an increasing trend along a NW–SE transect (Yao *et al.*, 2011; Yang *et al.*, 2015), the evolution of the spatial pattern of C_4 plant representation since the LGM is unclear.

Compared with previous work, our reconstruction of C_4 relative abundance is based on a greater number of sites ($n = 28$), covering the entire CLP, and it provides a detailed picture of the spatiotemporal evolution of C_4 plants since the LGM. The results indicate a significant increase in the representation of C_4 plants both temporally and spatially: for example, the C_4 representation increased from 8.6% during 21–19 ka bp to 26.1% during 10–6 ka bp (Fig. 2); in addition, the steepest spatial gradient in C_4 representation was during the early Holocene (~10–20% in the NW and ~40–60% in the SE; Figs 3 and S5).

Comparison of our reconstruction of the percentages of C_4 plants during the LGM and mid-Holocene with the results of other studies (Yao *et al.*, 2011; Yang *et al.*, 2015) reveals a general agreement that there was a significant NW–SE gradient in the representation of C_4 plants, as well as a significant increase in their representation throughout the CLP in the mid-Holocene, compared to the LGM. However, there are some differences: our reconstructed C_4 plant abundances during the LGM are ~5–10% higher than those of Yao *et al.* (2011) and Yang *et al.* (2015); however, our values for the mid-Holocene are ~10–20% lower than those of Yao *et al.* (2011) and are similar to those of Yang *et al.* (2015). In addition, our results indicate that, compared to the LGM, the percentage of C_4 plants increased by ~10% in the NW and ~30% in the SE, as is also suggested by Yang *et al.* (2015). In contrast, however, Yao *et al.* (2011) suggest a larger increase throughout the Plateau (~40%).

These disagreements can be explained by differences in the calculation of the end- member $\delta^{13}C$ values for C_3 and C_4 plants. For example, Yao *et al.* (2011) used values of −28.0 and −11.6‰ for $\delta^{13}C_{C3}$ and for $\delta^{13}C_{C4}$ during the mid-Holocene, respectively, and therefore their C_4 abundance values may be overestimated. By contrast, Yao *et al.* (2011) set the $\delta^{13}C_{C3}$ and $\delta^{13}C_{C4}$ values as −23.4 and −11.6‰ during the LGM, and thus the C_4 abundance values may be slightly underestimated. In contrast, in the present study, we used $\delta^{13}C$ values of modern plants from the CLP (Wang *et al.*, 2003, 2006, 2008; Liu *et al.*, 2005b), together with a consistent methodology (Table 1), which resulted in values of −24.1 and −10.0‰ for $\delta^{13}C_{C3}$ and $\delta^{13}C_{C4}$, respectively. Therefore, we suggest that our study has more robust end-members. In addition, the disagreements can be attributed to the fact that our dataset contains a larger number of loess–paleosol sites than those of Yao *et al.* (2011) (12 sites) and Yang *et al.* (2015) (21 sites). Thus, we suggest that overall our reconstruction provides a more accurate representation of the spatial distribution of C_4 plants across the CLP.

Our reconstruction of the evolution of the proportion of C_4 plants on the CLP since the LGM is also consistent with studies of the changing vegetation composition of the North American Great Plains, which indicate a much greater abundance of C_4 plants during the Holocene than during the LGM (e.g. Muhs *et al.*, 1999; Johnson and Willey, 2000). However, our results differ from most of the other studies of changes in C_4 plant abundance at low latitudes, which indicate a transition from C_4 dominance at the LGM to a mixture of C_3 and C_4 plants during the Holocene (e.g. Ficken *et al.*, 2002; Huang *et al.*, 2006; Castañeda *et al.*, 2007; Tierney *et al.*, 2010; Contreras-Rosales *et al.*, 2014).

In contrast to the ~1‰ ^{13}C-enriched organic matter in the paleosols, the isotopic signal of loess layers may be only slightly altered due to the lower degree of pedogenesis and the rapid burial of organic matter (Xie *et al.*, 2004; Obreht *et al.*, 2014). In this study, $\delta^{13}C$ values consistently represent an enrichment of ~3‰ in the upper parts of the mid-Holocene paleosol compared to the lower parts of the LGM loess unit in all studied sections (Figs S2–S4). This indicates that the variations in $\delta^{13}C$ values can be attributed to changes in the composition of the plant community. However, C_4 abundance during the last glacial may be slightly underestimated because we consistently corrected for SOM degradation by 1‰ in the loess layers, which is the same as for the paleosols. In addition, since carbon isotope fractionation in plants is greatly

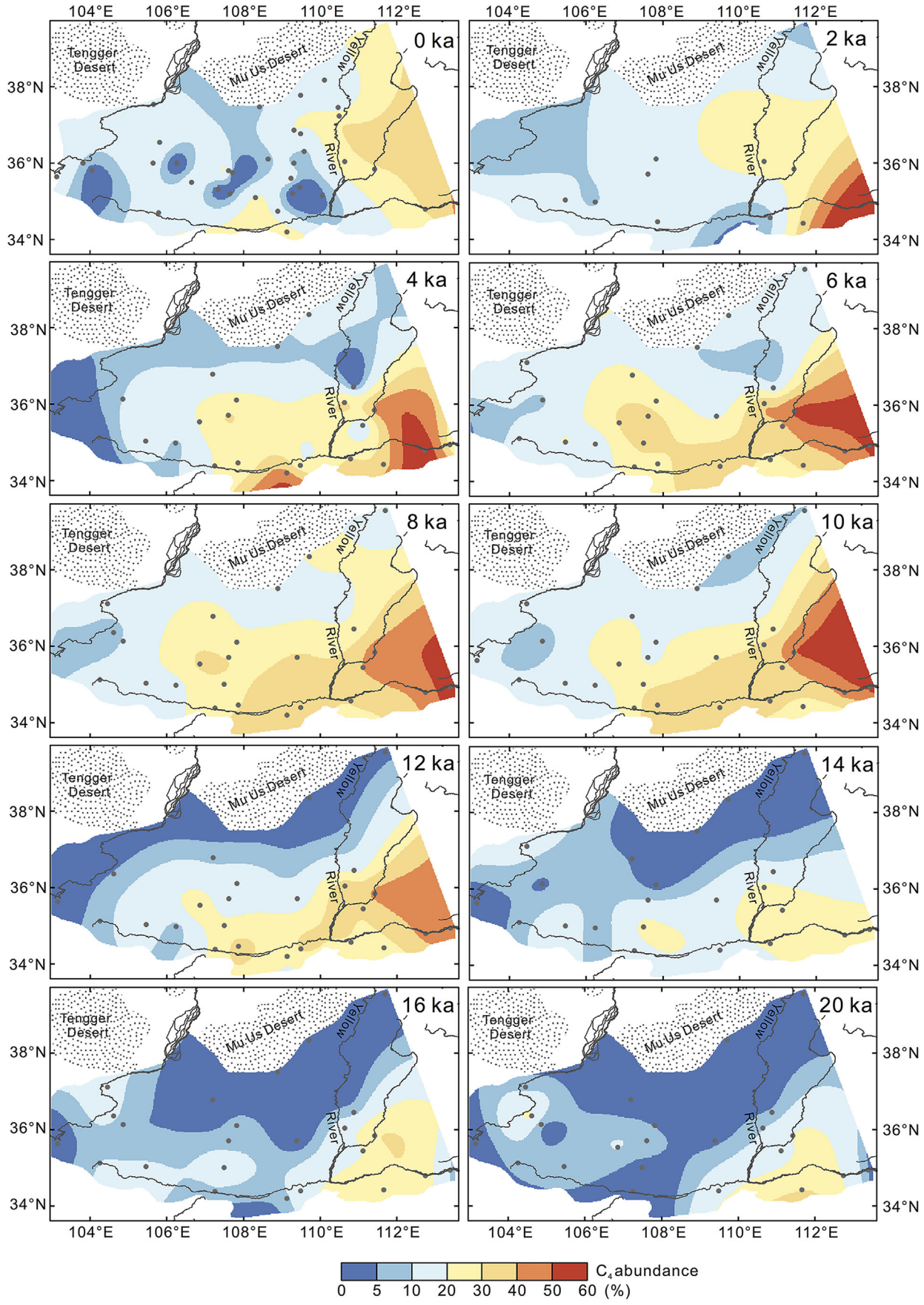

Figure 3. Time slices of the spatial distribution of the relative abundance of C_4 plants on the CLP since the LGM. Grey dots represent site locations.

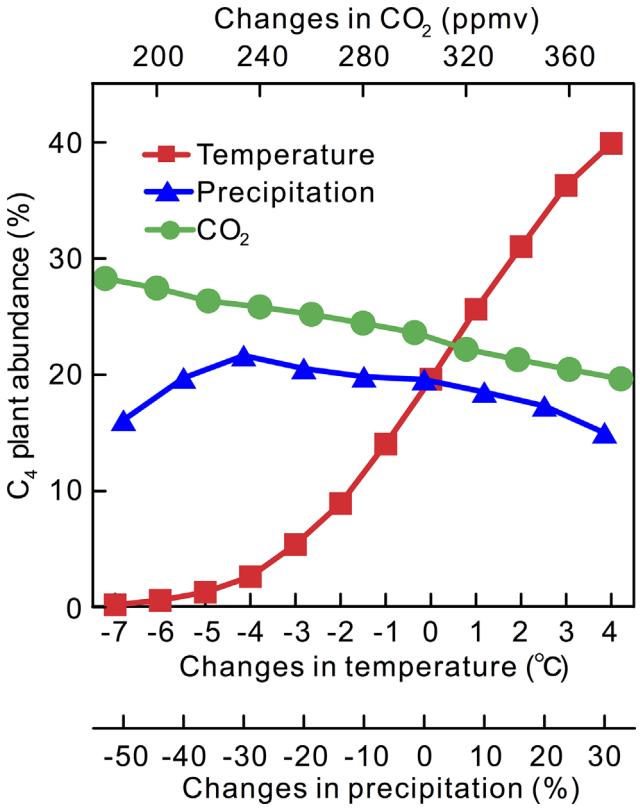

Figure 4. Results of a sensitivity analysis of the response of the relative abundance of C_4 plants across the CLP to changes in temperature (red squares), precipitation (blue triangles) and atmospheric CO_2 concentration (green circles). The BIOME4 model was run at a spatial resolution of $0.1 \times 0.1^{\circ}$.

affected by environmental factors (Farquhar *et al.*, 1989; Brugnoli and Farquhar, 2000), end-member $\delta^{13}C$ values of C_3 and C_4 plants are likely to have varied with changes in climate, atmospheric CO_2 level and $\delta^{13}C_{atm}$ since the LGM. However, we simplified the effect of environmental factors on our calculation of end-member values and assumed them to be constant through the past 21 ka. Therefore, the estimates of C_4 relative abundance presented herein are inevitably preliminary and there are some uncertainties.

Possible driving mechanism of the expansion of C_4 plants on the CLP since the LGM

Several factors, such as atmospheric CO_2 concentration, precipitation and temperature, can influence C_3 versus C_4 variability (Sage *et al.*, 1999). C_4 plants have developed a CO_2-concentrating mechanism and can suppress photorespiration at low CO_2/O_2 ratios and thus they are favored over C_3 plants under low CO_2 conditions (Collatz *et al.*, 1998; Raven *et al.*, 1999; Sage, 2001); notably, this in accord with the results of the sensitivity analysis in the present study (Fig. 4, green cycles). However, the reconstructed increase in C_4 abundance from the LGM to the Holocene was accompanied by an increase in atmospheric CO_2 content (Fig. 5b,d), which contradicts the results of the sensitivity analysis and plant physiology. Therefore, the expansion of C_4 plants on the CLP since the LGM may not have primarily been driven by CO_2 levels.

Two other factors have been invoked to explain changes in the proportion of C_4 plants during glacial–interglacial cycles on the CLP: first, the strengthening of the East Asian summer monsoon has been proposed as a major controlling factor (An *et al.*, 2005; Liu *et al.*, 2005a; Yao *et al.*, 2011; Yang *et al.*, 2015); and second, rising temperatures from glacial to interglacial have also been suggested to favor an increased proportion of C_4 plants (Gu *et al.*, 2003; Zhang *et al.*, 2003; Rao *et al.*, 2012).

Because the East Asian summer monsoon is characterized by synchronous changes in precipitation and temperature (Chen *et al.*, 1991), with higher precipitation and temperatures during interglacials, previous studies have found it difficult to distinguish their effects on C_4 plants. In the present study, we have attempted to distinguish the effects of temperature, precipitation and atmospheric CO_2 concentration on C_4 plant growth using a physiological process-based model. Our results reveal that C_4 abundance on the CLP is strongly positively correlated with increasing temperature since the LGM, and more weakly and negatively correlated with precipitation (Fig. 4). Undoubtedly, there are uncertainties in the simulation of the response of plants to environmental factors, including atmospheric CO_2, temperature and precipitation, using the coupled carbon and water flux scheme of the BIOME4 model. In addition, we compared the temporal variation of reconstructed percentages of C_4 plants with various climatic records (Fig. 5) to further determine the dominant factor affecting the expansion of C_4 plants on the CLP since the LGM.

A positive relationship between the temporal trend in C_4 abundance and precipitation (or effective moisture) reconstructions since the LGM is observed with increased C_4 abundance, corresponding to increased precipitation (Fig. 5c,d). However, it is clear that there is a phase difference in that increases in C_4 abundance lead those in precipitation. For example, a maximum in C_4 abundance occurred during the early Holocene, while the precipitation maximum occurred during the mid-Holocene. By contrast, the results of the sensitivity analysis indicate that C_4 plants have a competitive advantage over C_3 plants under arid conditions (less precipitation) (Fig. 4, blue triangles) because of their greater water-use efficiency (Raven *et al.*, 1999). However, the observed relationship between the temporal trends in the relative abundance of C_4 plants and paleoprecipitation (Fig. 5c,d), with increased C_4 abundance during wetter intervals, contradicts the results of previous studies. Therefore, we suggest that precipitation was not a dominant factor in the observed expansion of C_4 plants. Furthermore, our reconstruction of the spatial representation of C_4 plants indicates that they were less abundant in the relatively arid north-west CLP and more abundant in the more humid south-east, at all times (Figs 3 and S5). This further suggests that precipitation played only a relatively limited role in controlling the proportion of C_4 plants on the CLP.

Changes in the proportion of C_4 plants on the CLP are well correlated with temperature (Peterse *et al.*, 2011; Gao *et al.*, 2012; Shakun *et al.*, 2012; Marcott *et al.*, 2013) (Fig. 5a,d). There is an increase from the LGM to the early Holocene, which is followed by a subsequent decrease, despite a slight lead in summer insolation (Laskar *et al.*, 2004) relative to the record of C_4 abundance (Fig. 5b,d). Sensitivity analysis also revealed that C_4 abundance increased significantly with increasing temperature, and that temperature exerted a stronger control on C_4 plants than either atmospheric CO_2 or precipitation (Fig. 4). Therefore, our results support the conclusion that the expansion of C_4 plants since the LGM was mainly triggered by rising temperature.

Since global climate during the early Holocene was probably warmer than today (Shakun *et al.*, 2012; Marcott *et al.*, 2013), our finding that the highest abundance of C_4 plants on the CLP during the early Holocene was caused by increasing temperature is a potentially useful reference for a future warmer climate. From this long-term perspective

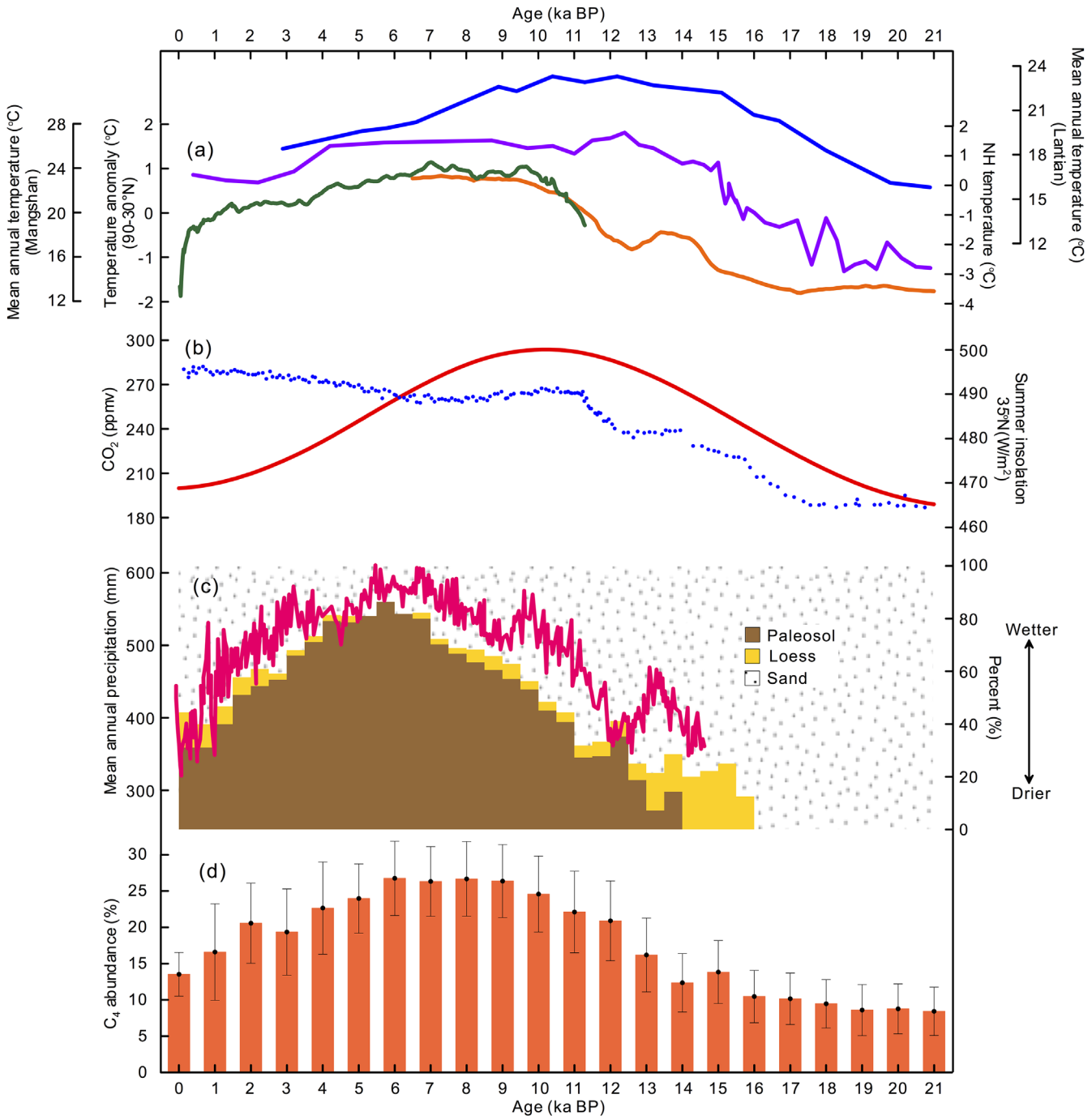

Figure 5. Comparison of the relative abundance of C_4 plants on the CLP with various climate proxy results since the LGM. (a) Reconstructed mean annual temperature at Mangshan (Peterse *et al.*, 2011) (purple line) and Lantian (Gao *et al.*, 2012) (blue line) on the CLP, changes in mean annual temperature at 30–90°N (Marcott *et al.*, 2013) (green line) and in the Northern Hemisphere (Shakun *et al.*, 2012) (orange line). (b) Summer insolation at 35°N (Laskar *et al.*, 2004) (red line) and atmospheric CO_2 concentration (Lüthi *et al.*, 2008) (blue dots). (c) History of effective moisture based on the sedimentary facies of the East Sandy lands in northern China (Li *et al.*, 2014), and an East Asian Summer Monsoon precipitation reconstruction based on pollen data from Gonghai Lake on the north-east margin of the CLP (Chen *et al.*, 2015) (red line). (d) Evolution of the relative abundance of C_4 plants on the CLP since the LGM (this study).

regarding the principal driver of C_4 plant abundance on the CLP, it is possible that the relative abundance of C_4 plants will increase as global warming continues.

Conclusions

We have combined 28 $\delta^{13}C$ records of SOM from loess–paleosol sequences and 34 $\delta^{13}C$ values of modern surface soils to reconstruct the spatiotemporal pattern of C_4 plant abundance across the CLP since the LGM. The results reveal that the relative abundance of C_4 plants generally increased since the LGM, reaching a maximum of 26.1% during 10–6 ka bp, then decreased during the late Holocene. Spatially, C_4 abundance was characterized by an increasing trend along a NW–SE transect across the CLP, with the steepest spatial gradient during the early Holocene.

Combined with the use of the BIOME4 model to study the sensitivity of C_4 plants to changes in climate and atmospheric CO_2 concentration, our results suggest that rising temperature was the dominant factor driving C_4 plant expansion on the CLP since the LGM; by contrast, precipitation and CO_2 concentration played a relatively limited role. On the basis of the present results, the relative abundance of C_4 plants on the CLP may increase in the future as global warming continues.

Acknowledgements. This research was funded by the National Basic Research Program of China (Grant No. 2016YFA0600504), the National Natural Science Foundation of China (Grant Nos. 41572165, 41430531, 41690114, 41125011 and 41502177), and the Bairen Programs of the Chinese Academy of Sciences.

Supporting Information

Additional supporting information may be found in the online version of this article at the publisher's web-site:

Text S1. Details of the age models and correlation of the sections.

Figure S1. Modern climate of the CLP.

Figure S2. Stratigraphic column, magnetic susceptibility (SUS), and $\delta^{13}C$ of soil organic matter for the selected loess sections across the CLP, and correlation with the chronologies of the Weinan-1 (Kang *et* al., 2011, 2013), Xifeng-1 (Lu *et al.*, 2006a), Luochuan-1 (Lu *et al.*, 2007), Lantian-1 (Lu *et al.*, 2006b) and Yuanbao-1 (Lai and Wintle, 2006).

Figure S3. Temporal changes in organic carbon isotope composition for the CLP since the LGM. Values are means, and error bars represent 95% confidence intervals.

Figure S4. Changes in the spatial distribution of carbon isotope values for the CLP at 1000-year intervals since the LGM. Grey cycles represent the location of data sites.

Figure S5. Changes in the spatial distribution of the relative abundance of C_4 plants on the CLP since the LGM. Grey circles represent the location of data sites.

Figure S6. Comparison of the carbon isotope values ($\delta^{13}C$) on the CLP with temperature, precipitation and magnetic susceptibility (MS).

Table S1. Characteristics of the carbon isotope data sites on the CLP.

Table S2. $\delta^{13}C$ data for surface soil and modern plants on the CLP.

Abbreviations. CLP, Chinese Loess Plateau; LGM, Last Glacial Maximum; MAP, mean annual precipitation; MAT, mean annual temperature; MS, magnetic susceptibility; OSL, optically stimulated luminescence; PFT, plant functional type; SOM, soil organic matter.

References

An ZS, Huang YS, Liu WG *et al.* 2005. Multiple expansions of C_4 plant biomass in East Asia since 7 Ma coupled with strengthened monsoon circulation. *Geology* **33**: 705–708.

Bartlein PJ, Harrison SP, Brewer S *et al.* 2011. Pollen-based continental climate reconstructions at 6 and 21 ka: a global synthesis. *Climate Dynamics* **37**: 775–802.

Bender MM. 1971. Variations in the $^{13}C/^{12}C$ ratios of plants in relation to the pathway of photosynthetic carbon dioxide fixation. *Phytochemistry* **10**: 1239–1244.

Briggs IC. 1974. Machine contouring using minimum curvature. *Geophysics* **39**: 39–48.

Brugnoli E, Farquhar GD. 2000. Photosynthetic fractionation of carbon isotopes. In *Photosynthesis: Physiology and Metabolism*, Leegood RC, Sharkey TD, Caemmerer SV (eds). Kluwer Academic Publishers: Dordrecht; 399–434.

Castañeda IS, Werne JP, Johnson TC. 2007. Wet and arid phases in the southeast African tropics since the Last Glacial Maximum. *Geology* **35**: 823–826.

Cerling TE. 1999. Stable carbon isotopes in palaeosol carbonates. *Palaeoweathering, Palaeosurfaces and Related Continental Deposits* **27**: 43–60.

Cerling TE, Harris JM, MacFadden BJ *et al.* 1997. Global vegetation change through the Miocene-Pliocene boundary. *Nature* **389**: 153–158.

Chen FH, Xu QH, Chen JH *et al.* 2015. East Asian summer monsoon precipitation variability since the last deglaciation. *Scientific Reports* **5**: 11186.

Chen LX, Zhu QG, Luo HB *et al.* 1991. *Monsoons over East Asia*. Meteorological Press: Beijing (in Chinese).

Clark PU, Dyke AS, Shakun JD *et al. 2009. The last glacial maximum. Science* **325**: 710–714.

Collatz GJ, Berry JA, Clark JS. 1998. Effects of climate and atmospheric CO_2 partial pressure on the global distribution of C_4 grasses: present, past, and future. *Oecologia* **114**: 441–454.

Contreras-Rosales LA, Jennerjahn T, Tharammal T *et al.* 2014. Evolution of the Indian Summer Monsoon and terrestrial vegetation in the Bengal region during the past 18 ka. *Quaternary Science Reviews* **102**: 133–148.

Diefendorf AF, Freeman KH, Wing SL *et al.* 2015. Paleogene plants fractionated carbon isotopes similar to modern plants. *Earth and Planetary Science Letters* **429**: 33–44.

Ehleringer JR, Cerling TE, Helliker BR. 1997. C_4 photosynthesis, atmospheric CO_2, and climate. *Oecologia* **112**: 285–299.

Farquhar GD. 1983. On the nature of carbon isotope discrimination in C_4 species. *Functional Plant Biology* **10**: 205–226.

Farquhar GD, Ehleringer JR, Hubick KT. 1989. Carbon isotope discrimination and photosynthesis. *Annual Review of Plant Physiology and Plant Molecular Biology* **40**: 503–537.

Ficken KJ, Wooller MJ, Swain DL *et al.* 2002. Reconstruction of a subalpine grass-dominated ecosystem, Lake Rutundu, Mount Kenya: a novel multi-proxy approach. *Palaeogeography, Palaeoclimatology, Palaeoecology* **177**: 137–149.

Food and Agriculture Organization (FAO). 1995. *Digital Soil Map of the World and Derived Soil Properties*. Food and Agriculture Organization: Rome.

Freyer HD, Belacy N. 1983. $^{13}C/^{12}C$ records in northern hemispheric trees during the past 500 years—anthropogenic impact and climatic superpositions. *Journal of Geophysical Research* **88**: 6844–6852.

Gao L, Nie JS, Clemens S *et al.* 2012. The importance of solar insolation on the temperature variations for the past 110 kyr on the Chinese Loess Plateau. *Palaeogeography, Palaeoclimatology, Palaeoecology* **317**: 128–133.

Gu ZY, Liu Q, Xu B *et al.* 2003. Climate as the dominant control on C_3 and C_4 plant abundance in the Loess Plateau: organic carbon isotope evidence from the last glacial-interglacial loess-soil sequences. *Chinese Science Bulletin* **48**: 1271–1276.

Guiot J, Cheddadi R, Prentice IC *et al.* 1996. A method of biome and land surface mapping from pollen data: application to Europe 6000 years ago. *Palaeoclimates: Data Model* **1**: 311–324.

Hatté C, Antoine P, Fontugne M *et al.* 2001. $\delta^{13}C$ of loess organic matter as a potential proxy for paleoprecipitation. *Quaternary Research* **55**: 33–38.

Hatté C, Guiot J. 2005. Palaeoprecipitation reconstruction by inverse modelling using the isotopic signal of loess organic matter: application to the Nußloch loess sequence (Rhine Valley, Germany). *Climate Dynamics* **25**: 315–327.

Heller F, Liu TS. 1984. Magnetism of Chinese loess deposits. *Geophysical Journal International* **77**: 125–141.

Huang YS, Shuman B, Wang Y *et al.* 2006. Climatic and environmental controls on the variation of C_3 and C_4 plant abundances in central florida for the past 62, 000 years. *Palaeogeography, Palaeoclimatology, Palaeoecology* **237**: 428–435.

Johnson WC, Willey KL. 2000. Isotopic and rock magnetic expression of environmental change at the Pleistocene-Holocene transition in the central Great Plains. *Quaternary International* **67**: 89–106.

Kang SG, Lu YC, Wang XL. 2011. Closely spaced recuperated OSL dating of the last interglacial paleosol in the southeastern margin of the Chinese Loess Plateau. *Quaternary Geochronology* **6**: 480–490.

Kang SG, Wang XL, Lu YC. 2013. Quartz OSL chronology and dust accumulation rate changes since the Last Glacial at Weinan on the southeastern Chinese Loess Plateau. *Boreas* **42**: 815–829.

Kaplan JO, Bigelow NH, Prentice IC. 2003. Climate change and Arctic ecosystems: 2. Modeling, paleodata-model comparisons, and future projections. *Journal of Geophysical Research* **108**: 1–12.

Kohn M. 2016. Carbon isotope discrimination in C_3 land plants is independent of nature variation in pCO_2. *Geochemical Perspectives Letters* **2**: 35–43.

Kukla G, An ZS. 1989. Loess stratigraphy in central China. *Palaeogeography, Palaeoclimatology, Palaeoecology* **72**: 203–225.

Kukla G, Heller F, Ming LX *et al.* 1988. Pleistocene climates in China dated by magnetic susceptibility. *Geology* **16**: 811–814.

Lai Z-P, Wintle AG. 2006. Locating the boundary between the Pleistocene and the Holocene in Chinese loess using luminescence. *Holocene* **16**: 893–899.

Laskar J, Robutel P, Joutel F *et al.* 2004. A long-term numerical solution for the insolation quantities of the Earth. *Astronomy and Astrophysics* **428**: 261–285.

Li Q, Wu HB, Yu YY *et al.* 2014. Reconstructed moisture evolution of the deserts in northern China since the Last Glacial Maximum and its implications for the East Asian Summer Monsoon. *Global and Planetary Change* **121**: 101–112.

Liu TS. 1985. *Loess and the Environment*. Science Press: Beijing (in Chinese).

Liu WG, Feng XH, Ning YF *et al.* 2005b. $\delta^{13}C$ variation of C_3 and C_4 plants across an Asian monsoon rainfall gradient in arid northwestern China. *Global Change Biology* **11**: 1094–1100.

Liu WG, Huang YS, An ZS *et al.* 2005a. Summer monsoon intensity controls C_4/C_3 plant abundance during the last 35 ka in the Chinese Loess Plateau: carbon isotope evidence from bulk organic matter and individual leaf waxes. *Palaeogeography, Palaeoclimatology, Palaeoecology* **220**: 243–254.

Liu WG, Ning YF, An ZS *et al.* 2002. Carbon isotopic composition of modern soil and paleosol as a response to vegetation change on the Chinese Loess Plateau. *Science in China Series D: Earth Sciences* **32**: 830–836 (in Chinese).

Liu WG, Yang H, Sun YB *et al.* 2011. $\delta^{13}C$ values of loess total carbonate: a sensitive proxy for Asian summer monsoon in arid northwestern margin of the Chinese loess plateau. *Chemical Geology* **284**: 317–322.

Lloyd J, Farquhar GD. 1994. $\delta^{13}C$ discrimination during CO_2 assimilation by the terrestrial biosphere. *Oecologia* **99**: 201–215.

Lu HY, Stevens T, Yi SW *et al.* 2006a. An erosional hiatus in Chinese loess sequences revealed by closely spaced optical dating. *Chinese Science Bulletin* **51**: 2253–2259.

Lu HY, Yi SW, Liu ZY *et al.* 2013. Variation of East Asian monsoon precipitation during the past 21 k. y. and potential CO_2 forcing. *Geology* **41**: 1023–1026.

Lu HY, Zhou YL, Mason J *et al.* 2006b. Late Quaternary Climatic changes in northern China-new evidences from sand dune and loess records based on optically stimulated luminescence dating. *Quaternary Sciences* **26**: 888–894 (in Chinese).

Lu YC, Wang XL, Wintle AG. 2007. A new OSL chronology for dust accumulation in the last 130, 000 yr for the Chinese Loess Plateau. *Quaternary Research* **67**: 152–160.

Lüthi D, Le Floch M, Bereiter B *et al.* 2008. High-resolution carbon dioxide concentration record 650,000-800,000 years before present. *Nature* **453**: 379–382.

Marcott SA, Shakun JD, Clark PU *et al.* 2013. A reconstruction of regional and global temperature for the past 11,300 years. *Science* **339**: 1198–1201.

Masson-Delmotte V, Schulz M, Abe-Ouchi A *et al.* 2013. Information from paleoclimate archives. In *Climate change 2013: the Physical Science Basis*, Stocker TF, Qin D, Plattner G-K *et al.* (eds). Cambridge University Press: Cambridge; 383–464.

Mauna Loa Observatory, 2000. ftp://aftp.cmdl.noaa.gov/data/trace_gases/co2c13/flask/surface/co2c13_mlo_surface-flask_1_sil_month.txt.

Melillo JM, Aber JD, Linkins AE *et al.* 1989. Carbon and nitrogen dynamics along the decay continuum: plant litter to soil organic matter. *Plant and Soil* **115**: 189–198.

Muhs DR, Aleinikoff JN, Stafford TW *et al.* 1999. Late Quaternary loess in northeastern Colorado: Part I-Age and paleoclimatic significance. *Geological Society of America Bulletin* **111**: 1861–1875.

Obreht I, Buggle B, Catto N *et al.* 2014. The Late Pleistocene Belotinac section (southern Serbia) at the southern limit of the European loess belt: environmental and climate reconstruction using grain size and stable C and N isotopes. *Quaternary International* **334–211**:10–19.

Peterse F, Prins MA, Beets CJ *et al.* 2011. Decoupled warming and monsoon precipitation in East Asia over the last deglaciation. *Earth and Planetary Science Letters* **301**: 256–264.

Qian LQ. 1991. *Climate in Loess Plateau*. China Meteorological Press: Beijing (in Chinese).

Rao ZG, Chen FH, Zhang X *et al.* 2012. Spatial and temporal variations of C_3/C_4 relative abundance in global terrestrial ecosystem since the Last Glacial and its possible driving mechanisms. *Chinese Science Bulletin* **57**: 4024–4035.

Raven PH, Evert RF, Eichhorn SE. 1999. *Biology of plants*. Freeman and Company Worth Publishers: New York; 126–153.

Sage RF. 2001. Environmental and evolutionary preconditions for the origin and diversification of the C_4 photosynthetic syndrome. *Plant Biology* **3**: 202–213.

Sage RF, Wedin DA, Li M. 1999. The biogeography of C_4 photosynthesis. In *C_4 plant biology*, Sage RF (ed.). Academic Press: New York; 313–373.

Schmitt J, Schneider R, Elsig J *et al.* 2012. Carbon isotope constraints on the deglacial CO_2 rise from ice cores. *Science* **336**: 711–714.

Schwartz D, Mariotti A, Lanfranchi R *et al.* 1986. $^{13}C/^{12}C$ ratios of soil organic matter as indicators of vegetation changes in the Congo. *Geoderma* **39**: 97–103.

Shakun JD, Clark PU, He F *et al.* 2012. Global warming preceded by increasing carbon dioxide concentrations during the last deglaciation. *Nature* **484**: 49–54.

Sheng CY. 1986. *A pandect of Chine climate*. Science Press: Beijing (in Chinese).

Shi YF, Kong ZZ, Wang SM *et al.* 1992. Climate fluctuations and important events during the Holocene warm period in China. *Science in China* **12**: 1300–1308 (in Chinese).

Stevens T, Lu HY. 2009. Optically stimulated luminescence dating as a tool for calculating sedimentation rates in Chinese loess: comparisons with grain-size records. *Sedimentology* **56**: 911–934.

Stewart GR, Turnbull MH, Schmidt S *et al.* 1995. ^{13}C natural abundance in plant communities along a rainfall gradient: a biological integrator of water availability. *Australian Journal of Plant Physiology* **22**: 51–55.

Stocker TF, Qin D, Plattner G-K *et al.* 2013. *IPCC, 2013: summary for policymakers. In Climate change 2013: the physical science basis*. Cambridge University Press: Cambridge; 3–29.

Tan ZH, Han YM, Cao JJ *et al.* 2015. Holocene wildfire history and human activity from high-resolution charcoal and elemental black carbon records in the Guanzhong basin of the Loess Plateau, China. *Quaternary Science Reviews* **109**: 76–87.

Tierney JE, Russell JM, Huang Y. 2010. A molecular perspective on Late Quaternary climate and vegetation change in the Lake Tanganyika basin, East Africa. *Quaternary Science Reviews* **29**: 787–800.

Van de Water PK, Leavitt SW, Betancourt JL. 2002. Leaf $\delta^{13}C$ variability with elevation, slope aspect, and precipitation in the southwest United States. *Oecologia* **132**: 332–343.

Vidic NJ, Montañez IP. 2004. Climatically driven glacial-interglacial variations in C_3 and C_4 plant proportions on the Chinese Loess Plateau. *Geology* **32**: 337–340.

Voelker SL, Brooks JR, Meinzer FC *et al.* 2016. A dynamic leaf gas-exchange strategy is conserved in woody plants under changing ambient CO_2: evidence from carbon isotope discrimination in paleo and CO_2 enrichment studies. *Global Change Biology* **22**: 889–902.

Wang GA. 2001. $\delta^{13}C$ ratios in herbaceous plants and surface soil organic matter in North China. PhD thesis, Chinese Academy of Sciences, China.

Wang G, Feng X, Han J *et al.* 2008. Paleovegetation reconstruction using $\delta^{13}C$ of soil organic matter. *Biogeosciences Discussions* **5**: 1795–1823.

Wang GA, Han JM, Liu DS. 2003. The carbon isotope composition of C_3 herbaceous plants in loess area of northern China. *Science in China Series D: Earth Sciences* **46**: 1069–1076.

Wang GA, Han JM, Zhou LP *et al.* 2006. Carbon isotope ratios of C_4 plants in loess areas of North China. *Science in China Series D* **49**: 97–102.

Wang GA, Li JZ, Liu XZ *et al.* 2013. Variations in carbon isotope ratios of plants across a temperature gradient along the 400 mm isoline of mean annual precipitation in north China and their relevance to paleovegetation reconstruction. *Quaternary Science Reviews* **63**: 83–90.

Wu NQ, Liu TS, Liu XP *et al.* 2002. Mollusk record of millennial climate variability in the Loess Plateau during the Last Glacial Maximum. *Boreas* **31**: 20–27.

Xie SC, Guo JQ, Huang JH *et al.* 2004. Restricted utility of $\delta^{13}C$ of bulk organic matter as a record of paleovegetation in some loess-Paleosol sequences in the Chinese Loess Plateau. *Quaternary Research* **62**: 86–93.

Yang SL, Ding ZL, Li YY *et al.* 2015. Warming-induced northwestward migration of the East Asian monsoon rain belt from the Last Glacial Maximum to the mid-Holocene. *Proceedings of the National Academy of Sciences of the United States of America* **112**: 13178–13183.

Yao Z, Wu H, Liang M *et al.* 2011. Spatial and temporal variations in C_3 and C_4 plant abundance over the Chinese Loess Plateau since the last glacial maximum. *Journal of Arid Environments* **75**: 881–889.

Yin LJ, Li MR. 1997. A study on the geographic distribution and ecology of C_4 plants in China. I. C_4 plant distribution in China and their relation with regional climatic condition. *Acta Ecologica Sinica* **17**: 350–363.

Zhang ZH, Zhao MX, Lu HY *et al.* 2003. Lower temperature as the main cause of C_4 plant declines during the glacial periods on the Chinese Loess Plateau. *Earth and Planetary Science Letters* **214**: 467–481 [DOI: 10.1016/S0012-821X(03)00387-X].